Published in final edited form as:

J Colloid Interface Sci. 2017 February 15; 488: 240–245. doi:10.1016/j.jcis.2016.10.093.

Rapid Microwave-Assisted Synthesis of sub-30 nm Lipid Nanoparticles

Stuart S. Dunn[a,b], **Denis R. Beckford Vera**[a,b], **S. Rahima Benhabbour**[c], and **Matthew C. Parrott**[a,b,d,*]

[a]Biomedical Research Imaging Center, University of North Carolina at Chapel Hill, NC, United States

[b]Department of Radiology, University of North Carolina at Chapel Hill, NC, United States

[c]Center for Nanotechnology in Drug Delivery, Division of Molecular Pharmaceutics, UNC Eshelman School of Pharmacy, United States

[d]The Carolina Institute for Nanomedicine, University of North Carolina at Chapel Hill, NC, United States

Abstract

Hypothesis—Accessing the phase inversion temperature by microwave heating may enable the rapid synthesis of small lipid nanoparticles.

Experiments—Nanoparticle formulations consisted of surfactants Brij 78 and Vitamin E TPGS, and trilaurin, trimyristin, or miglyol 812 as nanoparticle lipid cores. Each formulation was placed in water and heated by microwave irradiation at temperatures ranging from 65 °C to 245 °C. We observed a phase inversion temperature (PIT) for these formulations based on a dramatic decrease in particle Z-average diameters. Subsequently, nanoparticles were manufactured above and below the PIT and studied for (a) stability toward dilution, (b) stability over time, (c) fabrication as a function of reaction time, and (d) transmittance of lipid nanoparticle dispersions.

Findings—Lipid-based nanoparticles with distinct sizes down to 20–30 nm and low polydispersity could be attained by a simple, one-pot microwave synthesis. This was carried out by accessing the phase inversion temperature using microwave heating. Nanoparticles could be synthesized in just one minute and select compositions demonstrated high stability. The notable stability of these particles may be explained by the combination of van der Waals interactions and steric repulsion. 20–30 nm nanoparticles were found to be optically transparent.

Graphical abstract

*Corresponding author: Prof. Matthew C. Parrott, University of North Carolina at Chapel Hill, 2203 Marsico Building, 125 Mason Farm Rd., Chapel Hill, NC 27599-7513, Tel: + 1 919-966-3544, parrotmc@email.unc.edu.

Appendix A. Supplementary material

Supplementary data associated with this article can be found in the online version.

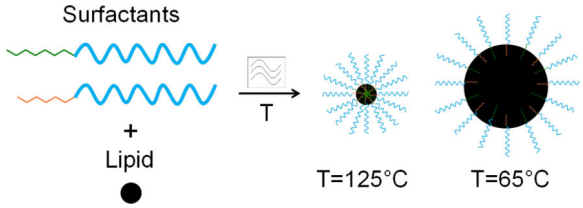

Keywords

Lipid nanoparticle; microwave synthesis; sub-30 nm; optical transparency

1. Introduction

The unique and wide-ranging properties of nanoparticles (NPs) have advanced numerous technologies. Ideal nanoparticle properties include low polydispersity for homogeneity, optical transparency for aesthetics, simple fabrication for scale-up, and physical stability for long-term application[1–3]. In addition, physical stability toward dilution is a critical property in drug delivery and cosmetics where NPs encounter notable changes in concentration. Nanoparticle size is a key property in determining behavior. For example, in sensing and analytical detection[4], [5], the light absorption and scattering properties of nanoparticles depend on size. Moreover, in nano-therapeutics, the size of NPs can influence blood circulation time, tissue targeting, drug release rate, and corresponding efficacy [6–9]. In cosmetics, skin hydration and absorption of active ingredients is influenced by nanoparticle size[10]. For food products, the color and appearance are crucial characteristics to consumers and depend on NP size[11], [12]. The importance of nanoparticle size can also be noted for catalysis[13, 14], pesticides[15, 16], and energy[17], [18] industries.

Many industries utilize lipid-based nanoparticles due to their biocompatibility, scalability, cheap raw materials, tunable cargo release, and the use of aqueous solvents in synthesis. Notable lipid-based nanoparticles include nanoemulsions and solid-lipid nanoparticles (SLNs). Lipid-based NPs consist of a core, liquid or solid, that is stabilized by surfactants. This yields stable dispersions with small sizes, large surface areas, and distinct core morphologies. Lipid NPs are typically made by high pressure homogenization, high shear homogenization, and ultrasonication[10], [19]. More recently, solid lipid nanoparticles (SLNs) have been prepared by a microemulsion-based technique using a Taguchi model of experimental design[20]. A follow-up study on this work involved the fabrication of these SLNs with microwave heating[21]. Compared to conventional heating, microwave heating yielded lower polydispersity particles with smaller sizes and a core-shell structure in a possible lamellar arrangement[22].

Microwave irradiation has also been utilized to synthesize nanoemulsions. For example, surfactant free emulsion polymerization was carried out for poly(methyl methacrylate) particles using microwave methodology[23]. Sub-50 nm crosslinked particles were obtained in a one-step process with good polydispersity. Another example involves the microwave-assisted synthesis of poly(ethylene glycol)-block-poly(styrene) emulsion nanoparticles,

which assumed smaller size and lower polydispersity when compared to conventional heating[24].

Smaller nanoparticles with lower polydispersity indices may be obtained by microwave synthesis on account of efficient localized heating and lower temperature gradients throughout the sample. Furthermore, microwave synthesis generally provides increased rates of reaction and product yields due to fast, homogeneous, and efficient dielectric heating[25]. In conventional heating, the vessel walls are heated first and then the heat diffuses into the reaction mixture. Conversely, microwave heating allows for higher temperatures to be reached rapidly by homogeneous heating of the entire reaction volume.

Here, we harness the advantages of microwave synthesis to influence the size of nanoparticles with a lipid-triglyceride core, both liquid and solid. Specifically, microwave heating was used to reduce lipid NP size. Small nanoparticles were tested for stability and scalability. We found an approach that is scalable and offers rapid synthesis of nanoparticles using biocompatible excipients. Furthermore, this approach provides a one-pot synthesis yielding purified nanoparticles directly from the microwave reactor. Nanoparticles with a lipid-triglyceride core, both liquid and solid, were rapidly fabricated using microwave heating. These nanoparticles had (1) small sizes depending on microwave conditions, (2) low polydispersity, (3) physical stability, and (4) optical transparency.

2. Experimental section

2.1 Materials

Polyoxyl 20-stearyl ether (Brij 78) was obtained from Uniqema (Wilmington, DE), d-alpha tocopheryl polyethylene glycol 1000 succinate (Vitamin E TPGS) was acquired from Eastman Chemicals (Kingsport, TN), and Miglyol 812 was purchased from Sasol (Witten, Germany) Trilaurin and trimyristin were purchased from Sigma Aldrich. Solvents were obtained from Thermo Fisher Scientific, Inc. Accessories for particle fabrication and analysis were obtained from Biotage and Thermo Fisher Scientific, Inc. The magnetic stir bars were made of ferrite and coated with poly(tetrafluoroethylene), and had a V-shape to fit the microwave vials. NP fabrication occurred in a Biotage® Initiator Classic microwave synthesizer. Dynamic light scattering occurred in a Zetasizer Nano ZS Particle Analyzer (Malvern Instruments, Inc.). % Transmittance was calculated from measurements on a SpectraMax M5 Plate Reader (Molecular Devices).

2.2 Synthesis of lipid-based particles

The formulation of nanoparticles was selected based on previous work[26, 27]. In a typical experiment, Brij 78, Vitamin E TPGS, and trilaurin were dissolved separately in chloroform to make stock solutions in 1.5 mL Eppendorf tubes. Aliquots were taken from the stock solutions containing 1.75 mg of Brij 78, 0.75 mg of Vitamin E TPGS, and 1.25 mg of trilaurin, which were added to a 0.5-2.0 mL microwave reaction vial and mixed by pipetting. The solvent was evaporated, yielding a film of the components. Filtered, deionized water (0.5 mL) was then added to the film to provide a 7.5 mg/mL concentration. The vial was charged with a magnetic stir bar and sealed with a microwave cap. The vial was then loaded

into the microwave synthesizer for a given time at a particular temperature using the very high absorption setting and fixed hold time (countdown starts after reaching the target temperature). All particles were synthesized in triplicate.

2.3 Characterization of lipid-based particles

The size of lipid-based particles was evaluated using Zetasizer Nano ZS Particle Analyzer (Malvern Instruments, Inc.). For the analysis of particles synthesized as a function of temperature and time, 0.5 mL of the particle dispersion in the microwave vial was directly aliquoted into a disposable microcuvette. Three measurements were taken for each particle sample using automatic measurement duration and 173° backscatter general purpose analysis model at 25 °C in water. We collected D_z, PDI, PDI width, and ζ-potential. The ζ-potential was measured on samples in 10 mM NaCl using a clear disposable zeta cell with automatic duration time, three measurements, and the Smoluchowski approximation.

2.4 Characterization of particle dilution

For the dilution studies, 0.5 mL of particles was diluted from 7.5 mg/mL to 2.5 mg/mL with water for the initial 3-fold dilution measurement. 100 μL of this initial solution was added to 900 μL water in a disposal cuvette to provide 30-fold dilution. For 150-fold dilution, 200 μL of the initial solution was added to 800 μL water. This was repeated out to a maximum of 30,000-fold dilution. The absolute percent change was determined for each particle based on the Z-average diameter at a particular dilution factor and the initial Z-average diameter at 7.5 mg/mL. The stability of nanoparticles was assessed from three different particle batches. Δ_{10} was calculated using one phase decay exponential fitting using GraphPad Prism software.

2.5 Characterization of stability over time

For the stability of particles over time, size measurements were taken after 1, 2, 3, and 4 weeks from the initial measurement using three different particle batches. Particles were stored at room temperature (23°C) at 7.5 mg/mL particle concentration in 1.5 mL Eppendorf tubes and dispensed into a disposable microcuvette for size analysis at each time point.

2.6 Characterization of particle transmittance

100 μL of 2.5 mg/mL particle dispersion was dispensed into 96-well clear-bottom plates. Absorbance measurements were taken every 10 nm from 400 nm to 700 nm using SpectraMax M5 Plate Reader (Molecular Devices). Three different batches of each unique NP type were measured and averaged. Percent transmittance was calculated from absorbance using the following equation: $A = 2 - \log(\%T)$ where A is the absorbance and %T is the percent transmittance. The average percent transmittance of each sample was presented by normalizing with water as the reference background.

3. Results and Discussion

3.1 Synthesis and characterization of lipid nanoparticles

To start we leveraged a nanoparticle composition previously reported[26, 27] due to its exceptional stability and simple fabrication. Furthermore, this nanoparticle composition was

scalable, efficacious in cancer treatment, and passed the National Cancer Institute's assay cascade [28–30]. Specifically, the lipid particle formulations were comprised of poly(ethylene glycol) surfactants (Vitamin E TPGS and Brij 78) and a lipid core. We selected the following three triglyceride lipids with unique alkyl chain lengths and different morphologies: miglyol 812 (liquid, T_m = −12.5 °C), trilaurin (solid, T_m = 46.5 °C), and trimyristin (solid, T_m = 56–57 °C). Nanoparticles were designated by the composition based on Brij 78, TPGS, and the lipid core. For example, a nanoparticle formulation consisting of **B**rij 78, vitamin E **T**PGS, and **M**iglyol would be denoted as **BTM**. Conventional heating of the BTM formulation at 65 °C for 30 minutes yielded 180-200 nm nanoparticles, which showed long circulation; however, these NPs may be too large to evade the reticuloendothelial system.

The three particle formulations investigated herein were abbreviated as BTM, BTL, and BTMy for **M**iglyol 812, tri**L**aurin, and tri**My**ristin cores, respectively. Lipid particles were synthesized via a one-pot approach using microwave irradiation. To determine the effect of reaction temperature on particle size, particles were synthesized at temperatures ranging from 65 °C to 245 °C in 20 °C increments (Figure S1) for 30 minutes. In general, at low (<125 °C) and high temperatures (>205 °C) nanoparticle size was large, while at intermediate temperatures, small nanoparticle sizes were accessible. This behavior may be explained by the phase inversion temperature (PIT) concept [31–34]. Phase inversion involves positive or negative spontaneous curvature changes in the surfactant during the emulsification process. At the PIT, the spontaneous curvature of the surfactant is zero, interfacial tension is low, and emulsion droplets are generally small.

For BTM and BTL formulations, microwave synthesis at 65 °C yielded nanoparticles sizes (D_z) of 190 nm and 280 nm, respectively (Figure 1b), with PDIs below 0.3. At 125 °C with microwave heating, small nanoparticles were obtained with D_z of 26 nm and 35 nm for BTM and BTL. The BTMy formulation showed no change in size regardless of temperature, and small nanoparticles could not be obtained at any temperature. The ζ-potential of BTM, BTL, and BTMy NPs synthesized under these conditions ranged from -3 mV to -5 mV (Table S2).

The inability of BTMy to reach small sizes may be attributed to lower affinity of the surfactant toward trimyristin due to its increased molecular weight and longer alkyl chains. The lower affinity of the surfactant toward the lipid combined with its larger size may influence the structures encountered at the PIT, hindering formation of small droplets. It could be possible to access 30 nm nanoparticles using more surfactant; however, this would drastically change the composition already established[22]. Given that we did not obtain smaller NP sizes with BTMy, we focused only on BTM and BTL NPs for subsequent experiments.

3.2 Stability of lipid nanoparticles toward dilution

The stability of each lipid nanoparticle was evaluated by monitoring the NP size in increasingly dilute conditions (Figure 2). If the NP size increased by 10% of the original size we considered the system unstable. We called this number delta-10 (Δ_{10}). An estimated dilution factor and particle concentration was calculated at the delta-10 (Table 1). The higher

the dilution factor, the more stable the NP. Similarly, the lower the particle concentration, the more stable the NP. These dilution stability assays are relevant in cosmetics and drug delivery applications where particles are subjected to large changes in concentration. For example, in drug-delivery, intravenous injection of nanoparticles will be subjected to an instant dilution of 10-100x immediately after injection. Therefore, the stability towards this degree of dilution is of utmost importance. BTM and BTL NPs prepared at 65 °C and 125 °C were analyzed for dilution stability.

The nanoparticles are designated by preparation temperature. For example, BTL_{65} represents trilaurin-based NPs fabricated at 65 °C. Consistently, we found that NPs prepared at 65 °C were more stable than NPs fabricated at 125 °C. For instance, the Δ_{10} dilution factor for BTM_{65} (2016x) was roughly 12 times higher than that of BTM_{125} (162x). Similarly, the Δ_{10} dilution factor for BTL_{65} was 27 times higher than that of BTL_{125}. BTL_{65} showed the greatest stability, which may be due to it having the largest Z-average diameter. In these studies, smaller particles were found to be less stable toward dilution than larger nanoparticles, which may be attributed to the difference in surface area to volume ratios. However, these small nanoparticles were still very stable and could withstand a 100-fold dilution. The stability of these nanoparticles may be attributed to van der Waals attraction and steric repulsion, which arises with nonionic surfactants[32]. The size of the diluted nanoparticles may increase over time due to surfactant desorption, Oswald ripening, and coalescence. Long-term stability of diluted nanoparticles may be realized by adding glycerol or ionic surfactants as noted in literature [35, 36].

3.3 Stability of lipid nanoparticles over time

In addition to the stability of the nanoparticles toward dilution, the stability of lipid nanoparticles over time was investigated. This was completed by monitoring their size over four weeks at one week intervals (Figure 3). We observed that BTL NPs showed smaller changes in size than BTM NPs over 4 weeks. For example, BTM_{125} increased 13 nm while BTL_{125} changed less than 1 nm after 4 weeks. Similarly, BTM_{65} NPs changed 21 nm in diameter while BTL_{65} changed 3 nm after 4 weeks. Statistical analysis was performed on lipid nanoparticles comparing the initial measurement with each week time point. The changes in particle size were significant ($p<0.05$) for both BTM NPs using a t-test. Conversely, BTL particles did not show significant fluctuations in size based on a similar t-test. Solid core NPs were more stable over time than liquid core NPs, which may be attributed to the different lipid morphologies.

3.4 Synthesis of lipid nanoparticles as a function of time

To facilitate rapid production of these lipid-based particles for potential applications, the effect of reaction time on particle size was studied. Conventional approaches to fabricate lipid-based nanoparticles require 30 min[26, 27]. Herein, reaction times of 30 min, 10 min, 5 min, and 1 min were utilized at 65 °C and 125 °C (Figure 4). Short reaction times facilitate scale-up, which is important for industrial applications. In just 1 minute, and for the first time, BTM nanoparticles could be synthesized at 65 °C and 125 °C to provide sub-30 nm nanoparticles. Across all reaction times, small BTM_{125} NPs were observed with diameters less than 32 nm and were statistically similar. BTMs responded particularly well to high

temperatures at short times. The microwave-assisted synthesis of both large and small BTM nanoparticles demonstrates potential for rapid scale-up.

Larger BTL particles could be synthesized in 1 minute at 65 °C with statistically similar sizes down to 5 min. Conversely, smaller BTL nanoparticles could not be synthesized at short times at 125 °C, and still required 30 minutes of microwave heating. The difference in particle size versus microwave time is attributed to core morphology. Specifically, longer time is required to melt the solid trilaurin lipid and reach equilibrium with the surfactants to access the PIT. Once in a nanoemulsion state with the lipid melted, it is possible to form small BTL nanodroplets. This small nanoparticle state in the PIT is maintained post-fabrication since the microwave synthesizer rapidly cools the reaction after completion and solidifies the trilaurin lipid core.

The transparency of lipid-based nanoparticles was studied over the visible wavelength spectrum (Figure 5). The transparency of nanoparticles finds importance in a variety of technologies such as coatings and cosmetics for aesthetic characteristics. For example, sunscreen formulations favor transparent nanoparticles, antioxidants, and UV absorbers (filters[37]). This lipid-based nanoparticle formulation utilizes vitamin E, which is both an antioxidant and UV absorber, making these nanoparticles ideal for sunscreens and other cosmetics.

3.5 Transmittance of lipid nanoparticles

Optical transparency from 400-700 nm was observed for small nanoparticles fabricated at 125 °C (BTM_{125} and BTL_{125}). Distinct transmittance profiles were observed for larger particles with the percent transmittance (%*T*) ranging from 35% to 86%. At 500 nm, the %T of BTM_{65} was 1.5 times higher than that of BTL_{65} (Table 2). This is attributed to the larger size of BTL_{65} NPs, which will absorb more light. Distinct transmittance profiles, including optical transparency, were provided for lipid-based nanoparticles by this microwave-assisted synthetic approach.

4. Conclusions

Through our investigations we were able to control the preparation of lipid-based nanoparticles using microwave heating, and fabricate small nanoparticles in unprecedented reaction times. Previously, microwave heating has been utilized to prepare lipid-based nanoparticles with diameters between 100 nm to 300 nm in 10 minutes [21, 22, 38]. Furthermore, the phase inversion temperature (PIT) method has been reported [31–34] to show nanoparticle sizes below 100 nm [39–42]. We selected a formulation that has been used to prepare ~200 nm nanoparticles with the ability to target tumors, deliver chemotherapeutic drugs *in vivo* and overcome multidrug resistance [26–30]. For the first time, we have demonstrated the feasibility in accessing the PIT method by microwave heating to yield sub-30 nm nanoparticles. Moreover, these nanoparticles are physically stable, optically transparent, and can be fabricated in 1 minute. These improvements are not possible using conventional thermal heating [27]. To the best of our knowledge, this is the first demonstration of 20–30 nm lipid nanoparticles fabricated by microwave irradiation using this formulation. Future work utilizing the PIT-microwave heating approach may be

applied to a range of colloidal systems involving different surfactants and lipids to access smaller nanoparticle sizes in faster times for a variety of applications. Specifically, the rapid synthesis of 20–30 nm nanoparticles presented herein may allow for enhanced tumor targeting, drug delivery efficacy, and scalability toward potential clinical application. Tumor targeting and drug delivery efficacy may be enhanced by using 20–30 nm NPs as this size range has been shown to have the longest blood circulation half life and highest tumor accumulation[43].

Supplementary Material

Refer to Web version on PubMed Central for supplementary material.

Acknowledgments

The project described was supported by the National Center for Advancing Translational Sciences, National Institutes of Health, through Grant 1KL2TR001109. The content is solely the responsibility of the authors and does not necessarily represent the official views of the NIH.

Abbreviations

NPs	Nanoparticles
T_m	melting temperature
BTM, BTL, or BTMy	**B**rij 78, vitamin E **T**PGS, and **M**iglyol 812, tri**L**aurin, or tri**My**ristin
delta-10 (Δ_{10})	the point at which particle size increased by 10%
$BTM_{65/125}$	BTM NPs fabricated at 65 °C or 125 °C;
$BTL_{65/125}$	BTL NPs fabricated at 65 °C or 125 °C;
D_z	Z-average diameter
PDI	polydispersity index
n.s.	not significant

References

1. Majuru, MO.; Oyewumi, S. Nanotechnology in Drug Development and Life Cycle Management. In: de Villiers, GS.; Aramwit, MM.; Kwon, P., editors. Nanotechnol. Drug Deliv. 1st. New York: Springer-Verlag; 2009. p. 597-619.
2. Cutts SM, Evison BJ, Pigram PJ. Factors determining the stability, size distribution, and cellular accumulation of small, monodisperse chitosan nanoparticles as candidate vectors for anticancer drug delivery: application to the passive encapsulation of [14C] - doxorubicin. Nanotechnol. Sci. Appl. 2015; 8:67–80. [PubMed: 26715842]
3. Faure B, Salazar-Alvarez G, Ahniyaz A, Villaluenga I, Berriozabal G, De Miguel YR, Bergström L. Dispersion and surface functionalization of oxide nanoparticles for transparent photocatalytic and UV-protecting coatings and sunscreens. Sci. Technol. Adv. Mater. 2013; 14:23001.
4. Orendorff CJ, Sau TK, Murphy CJ. Shape-Dependent Plasmon-Resonant Gold Nanoparticles. Small. 2006; 2:636–639. [PubMed: 17193100]

5. Van Duyne RP, Haes AJ, McFarland AD. Nanoparticle optics: sensing with nanoparticle arrays and single nanoparticles. Proc. SPIE. 2003; 5223:197–207.
6. Choi HS, Liu W, Misra P, Tanaka E, Zimmer JP, Itty Ipe B, Bawendi MG, Frangioni JV. Renal clearance of quantum dots. Nat. Biotechnol. 2007; 25:1165–1170. [PubMed: 17891134]
7. Albanese A, Tang PS, Chan WCW. The Effect of Nanoparticle Size, Shape, and Surface Chemistry on Biological Systems. Annu. Rev. Biomed. Eng. 2012; 14:1–16. [PubMed: 22524388]
8. Wang AZ, Langer R, Farokhzad OC. Nanoparticle Delivery of Cancer Drugs. Annu. Rev. Med. 2012; 63:185–198. [PubMed: 21888516]
9. Wang L, Dong J, Chen J, Eastoe J, Li X. Design and optimization of a new self-nanoemulsifying drug delivery system. J. Colloid Interface Sci. 2009; 330:443–448. [PubMed: 19038395]
10. Puglia C, Bonina F. Lipid nanoparticles as novel delivery systems for cosmetics and dermal pharmaceuticals. Expert Opin. Drug Deliv. 2012; 9:429–441. [PubMed: 22394125]
11. McClements DJ, Chantrapornchai W, Clydesdale F. Prediction of Food Emulsion Color Using Light Scattering Theory. J. Food Sci. 2006; 63:935–939.
12. Weiss J, Liao W. Addition of sugars influences color of oil-in-water emulsions. J. Agric. Food Chem. 2000; 48:5053–5060. [PubMed: 11052777]
13. Guo S, Zhang S, Sun S. Tuning Nanoparticle Catalysis for the Oxygen Reduction Reaction. Angew. Chemie Int. Ed. 2013; 52:8526–8544.
14. Yan N, Xiao C, Kou Y. Transition metal nanoparticle catalysis in green solvents. Coord. Chem. Rev. 2010; 254:1179–1218.
15. Wang L, Li X, Zhang G, Dong J, Eastoe J. Oil-in-water nanoemulsions for pesticide formulations. J. Colloid Interface Sci. 2007; 314:230–235. [PubMed: 17612555]
16. Paul B, Locke A, Martens WN, Frost RL. Decoration of titania nanofibres with anatase nanoparticles as efficient photocatalysts for decomposing pesticides and phenols. J. Colloid Interface Sci. 2012; 386:66–72. [PubMed: 22909968]
17. Saunders BR, Turner ML. Nanoparticle–polymer photovoltaic cells. Adv. Colloid Interface Sci. 2008; 138:1–23. [PubMed: 17976501]
18. Lee S, Cho Y, Song H-K, Lee KT, Cho J. Carbon-Coated Single-Crystal LiMn2O4 Nanoparticle Clusters as Cathode Material for High-Energy and High-Power Lithium-Ion Batteries. Angew. Chemie Int. Ed. 2012; 51:8748–8752.
19. Solans C, Solé I. Nano-emulsions: Formation by low-energy methods. Curr. Opin. Colloid Interface Sci. 2012; 17:246–254.
20. Shah R, Eldridge D, Palombo E, Harding I. Optimisation and stability assessment of solid lipid nanoparticles using particle size and zeta potential. J. Phys. Sci. 2014; 25:59–75.
21. Shah RM, Malherbe F, Eldridge D, Palombo Ea, Harding IH. Physicochemical characterization of solid lipid nanoparticles (SLNs) prepared by a novel microemulsion technique. J. Colloid Interface Sci. 2014; 428:286–294. [PubMed: 24910064]
22. Shah RM, Bryant G, Taylor M, Eldridge DS, Palombo EA, Harding IH. Structure of solid lipid nanoparticles produced by a microwave-assisted microemulsion technique. R. Soc. Chem. Adv. 2016; 6:36803–36810.
23. An Z, Tang W, Hawker CJ, Stucky GD. One-step microwave preparation of well-defined and functionalized polymeric nanoparticles. J. Am. Chem. Soc. 2006; 128:15054–15055. [PubMed: 17117833]
24. Xu Z, Hu X, Li X, Yi C. Monodispersed PEG-b-PSt Nanoparticles. J. Polym. Sci. Part A Polym. Chem. 2007; 46:481–488.
25. Horikoshi, S.; Serpone, N. Microwaves in Nanoparticle Synthesis. 1st. KGaA, Weinheim, Germany: Wiley-VCH Verlag GmbH & Co.; 2013.
26. Benhabbour SR, Luft JC, Kim D, Jain A, Wadhwa S, Parrott MC, Liu R, DeSimone JM, Mumper RJ. In vitro and in vivo assessment of targeting lipid-based nanoparticles to the epidermal growth factor-receptor (EGFR) using a novel Heptameric ZEGFR domain. J. Control. Release. 2012; 158:63–71. [PubMed: 22037106]

27. Dong X, Mattingly CA, Tseng M, Cho M, Adams VR, Mumper RJ. Development of new lipid-based paclitaxel nanoparticles using sequential simplex optimization. Eur. J. Pharm. Biopharm. 2009; 72:9–17. [PubMed: 19111929]
28. Ma P, Benhabbour SR, Peng L, Mumper RJ. 2-Behenoyl-paclitaxel conjugate containing lipid nanoparticles for the treatment of metastatic breast cancer. Cancer Lett. 2013; 334:253–262. [PubMed: 22902506]
29. Peng L, Feng L, Yuan H, Benhabbour SR, Mumper RJ. Development of a novel orthotopic non-small cell lung cancer model and therapeutic benefit of 2'-(2-bromohexadecanoyl)-docetaxel conjugate nanoparticles. Nanomedicine Nanotechnology, Biol. Med. 2014; 10:1497–1506.
30. Dong X, Mattingly CA, Tseng MT, Cho MJ, Liu Y, Adams VR, Mumper RJ. Doxorubicin and paclitaxel-loaded lipid-based nanoparticles overcome multidrug resistance by inhibiting P-glycoprotein and depleting ATP. Cancer Res. 2009; 69:3918–3926. [PubMed: 19383919]
31. Fernandez P, André V, Rieger J, Kühnle A. Nano-emulsion formation by emulsion phase inversion. Colloids Surfaces A Physicochem. Eng. Asp. 2004; 251:53–58.
32. Tadros, TF. Emulsion Formation and Stability. 1st. KGaA, Weinheim, Germany: Wiley-VCH Verlag GmbH & Co.; 2013.
33. Shinoda K, Saito H. The Stability of O/W type emulsions as functions of temperature and the HLB of emulsifiers: The emulsification by PIT-method. J. Colloid Interface Sci. 1969; 30:258–263.
34. Shinoda K, Saito H. The effect of temperature on the phase equilibria and the types of dispersions of the ternary system composed of water, cyclohexane, and non-ionic surfactant. J. Colloid Interface Sci. 1968; 26:70–74.
35. Wang L, Tabor R, Eastoe J, Li X, Heenan RK, Dong J. Formation and stability of nanoemulsions with mixed ionic-nonionic surfactants. Phys. Chem. Chem. Phys. 2009; 11:9772–9778. [PubMed: 19851556]
36. Saberi AH, Fang Y, McClements DJ. Effect of glycerol on formation, stability, and properties of vitamin-E enriched nanoemulsions produced using spontaneous emulsification. J. Colloid Interface Sci. 2013; 411:105–113. [PubMed: 24050638]
37. Puglia C, Damiani E, Offerta A, Rizza L, Tirendi GG, Tarico MS, Curreri S, Bonina F, Perrotta RE. Evaluation of nanostructured lipid carriers (NLC) and nanoemulsions as carriers for UV-filters: Characterization, in vitro penetration and photostability studies. Eur. J. Pharm. Sci. 2014; 51:211–217. [PubMed: 24157543]
38. Shah RM, Rajasekaran D, Ludford-menting M, Eldridge DS, Palombo EA, Harding IH. Colloids and Surfaces B : Biointerfaces Transport of stearic acid-based solid lipid nanoparticles (SLNs) into human epithelial cells. Colloids Surfaces B Biointerfaces. 2016; 140:204–212. [PubMed: 26764103]
39. Izquierdo P, Esquena J, Tadros TF, Dederen JC, Feng J, Garcia-Celma MJ, Azemar N, Solans C. Phase behavior and nano-emulsion formation by the phase inversion temperature method. Langmuir. 2004; 20:6594–6598. [PubMed: 15274560]
40. Izquierdo P, Feng J, Esquena J, Tadros TF, Dederen JC, Garcia MJ, Azemar N, Solans C. The influence of surfactant mixing ratio on nano-emulsion formation by the pit method. J. Colloid Interface Sci. 2005; 285:388–394. [PubMed: 15797437]
41. Izquierdo P, Esquena J, Tadros TF, Dederen C, Garcia MJ, Azemar N, Solans C. Formation and stability of nano-emulsions prepared using the phase inversion temperature method. Langmuir. 2002; 18:26–30.
42. Morales D, Gutiérrez JM, García-Celma MJ, Solans YC. A study of the relation between bicontinuous microemulsions and oil/water nano-emulsion formation. Langmuir. 2003; 19:7196–7200.
43. Perrault CW, Walkey SD, Jennings C, Fischer HC T. Mediating tumor targeting efficiency of nanoparticles through design. Nano Lett. 2009; 9:1909–1915. [PubMed: 19344179]

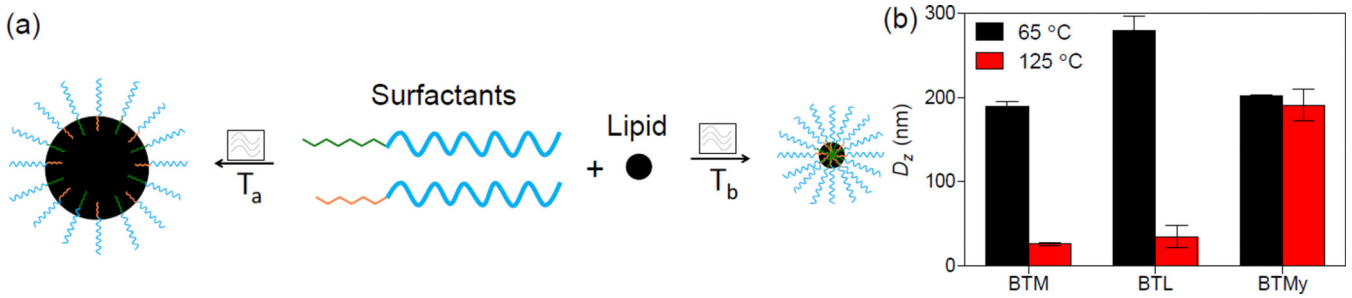

Figure 1.

(a) Schematic of lipid nanoparticles with different sizes synthesized at microwave temperatures T_a or T_b. (b) Z-average diameter (D_z) of BTM, BTL, and BTMy nanoparticles synthesized at 65 °C and 125 °C for 30 min. Error bars represent ± the standard deviation over 3 measurements.

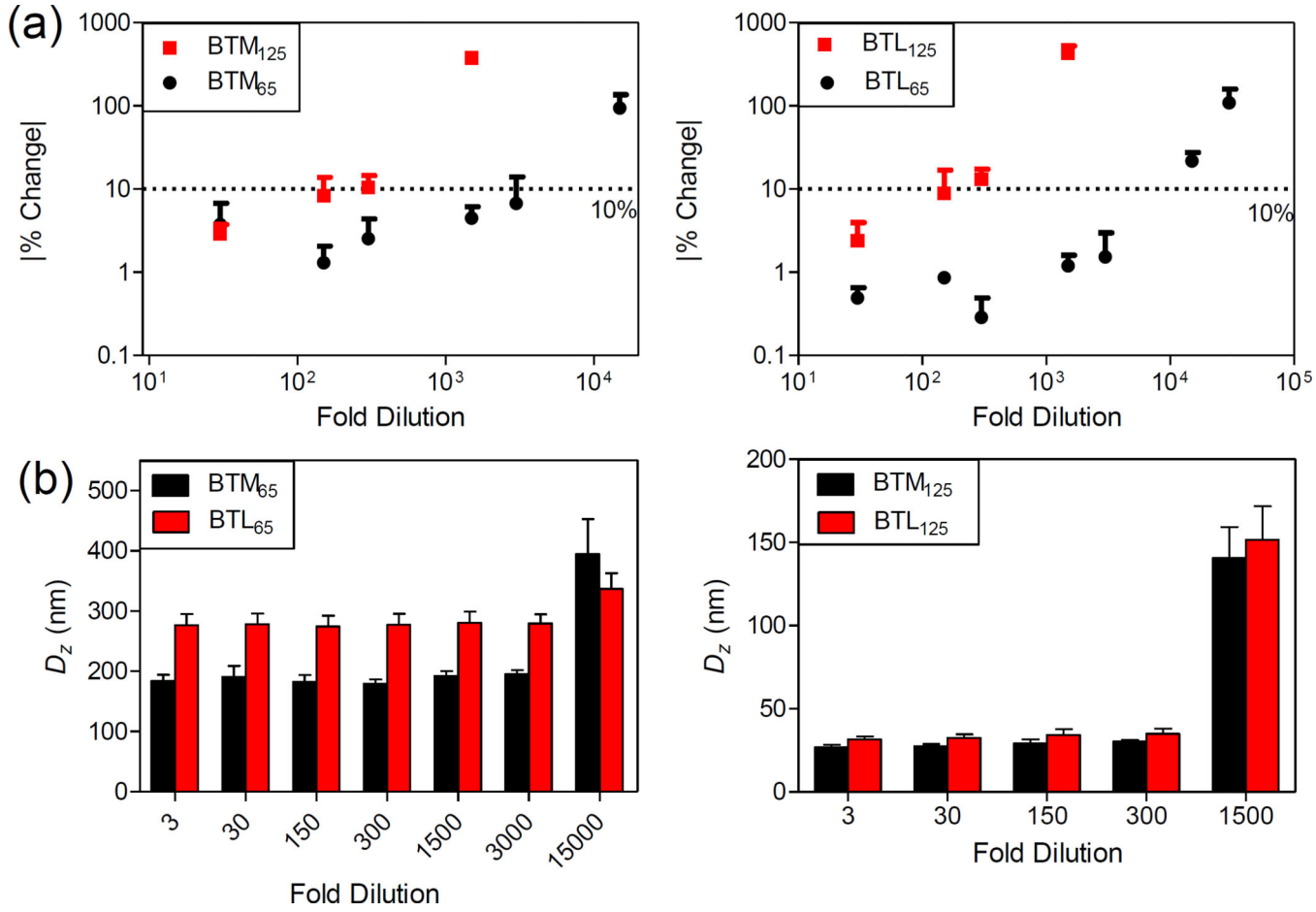

Figure 2.

(a) Absolute percent change of Z-average diameter and (b) size stability of BTM and BTL NPs synthesized at 65 °C or 125 °C for 30 min as a function of dilution. Error bars represent ± the standard deviation over 3 measurements.

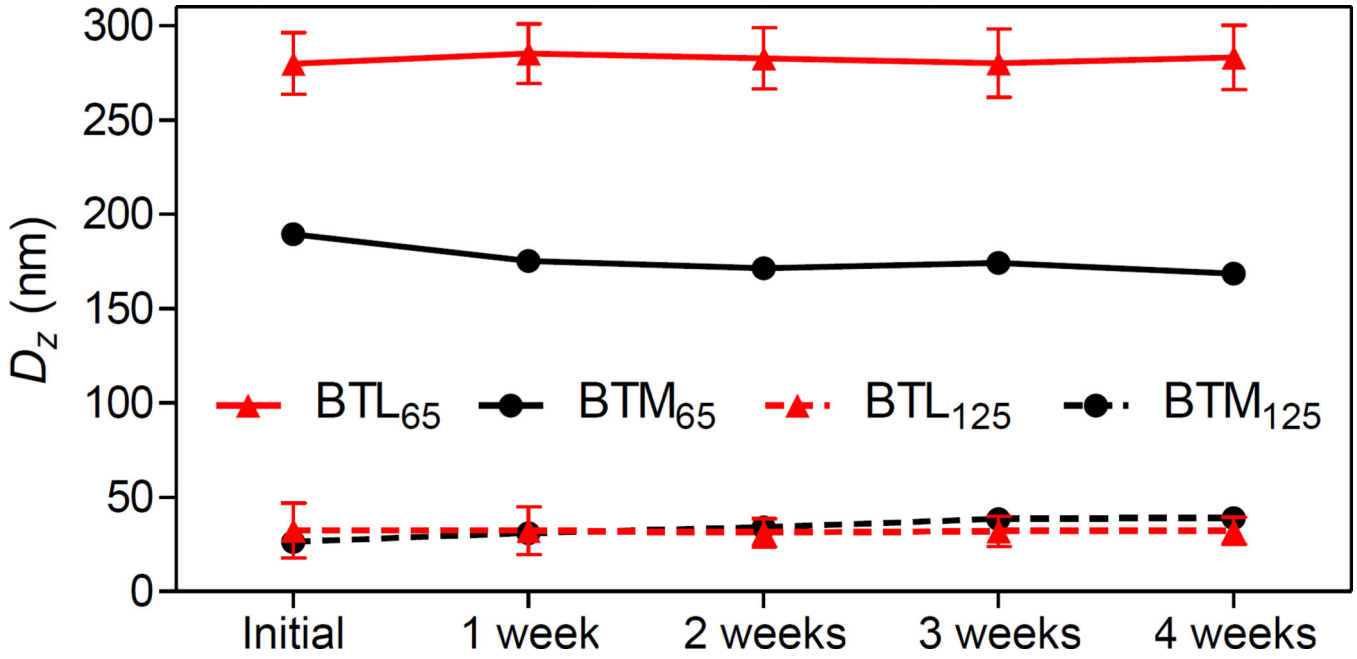

Figure 3.

Stability of BTM and BTL lipid nanoparticles synthesized at 65 °C or 125 °C for 30 min over four weeks in one week intervals. Error bars represent ± the standard deviation over 3 measurements.

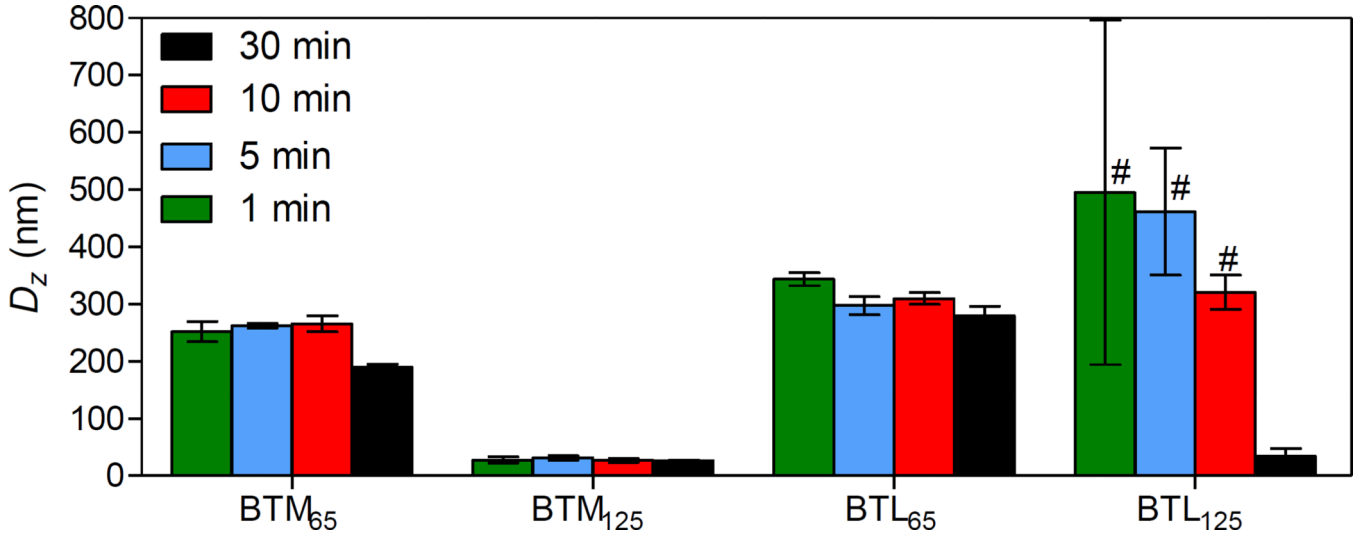

Figure 4.

Z-average diameter of lipid particles as a function of reaction time. Error bars represent ± the standard deviation over 3 measurements. #Some samples consisted of more than one peak in dynamic light scattering.

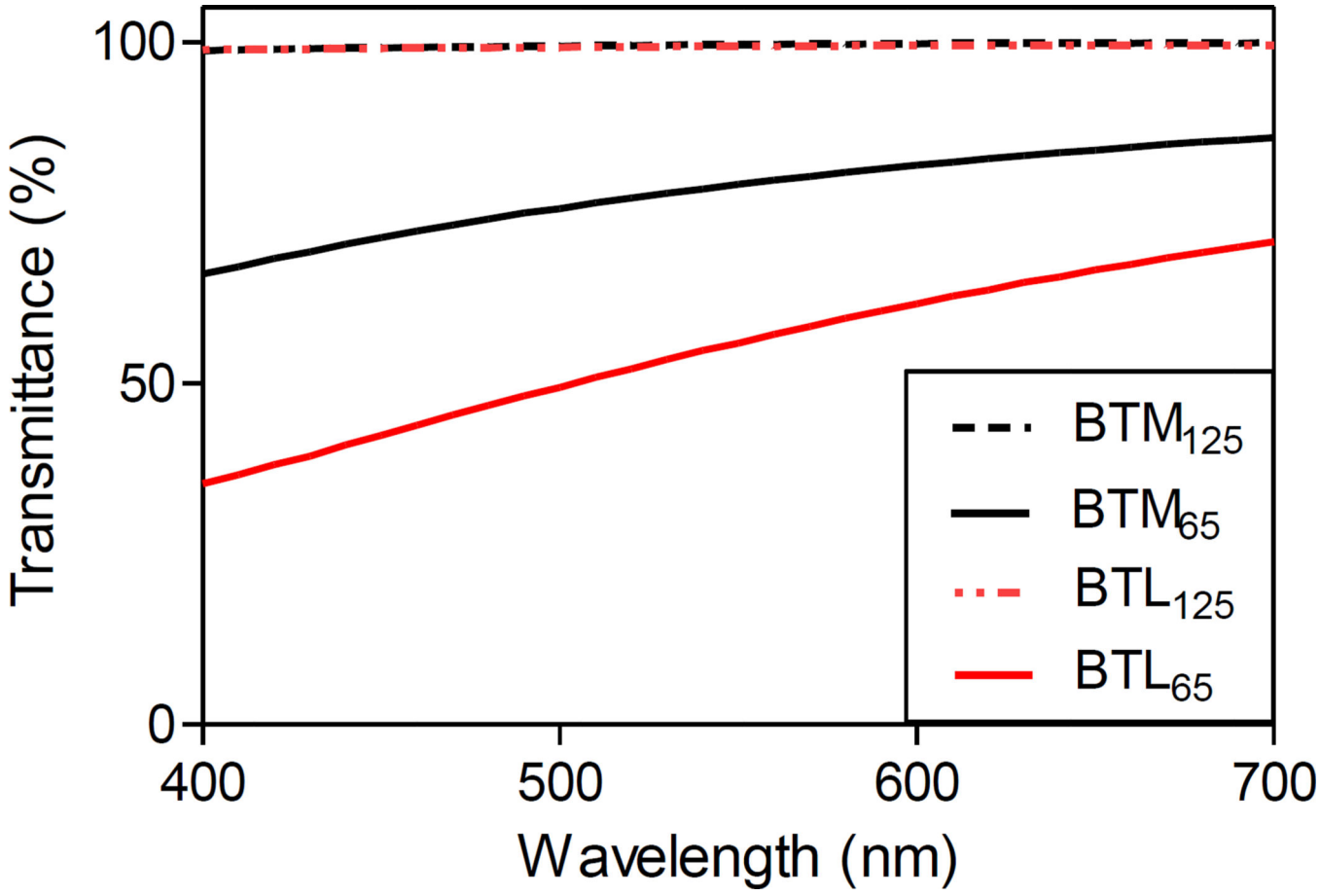

Figure 5.
Transmittance of lipid nanoparticles synthesized at 65 °C or 125 °C for 30 min over the visible wavelength spectrum. Small nanoparticles are optically transparent while large particles exhibit distinct transmittance profiles.

Table 1

Dilution factor and concentration at the Δ_{10} of each nanoparticle with Z-average diameter (D_z) ± the standard deviation over 3 measurements.

Particle	Dilution factor	Concentration (μg/mL)	D_z
BTM_{65}	2016x	1.2	189.5 ± 5.7
BTM_{125}	162x	15.4	26.1 ± 1.6
BTL_{65}	4404x	0.6	280.0 ± 16.3
BTL_{125}	159x	15.7	34.6 ± 12.9

Table 2

Percent transmittance (%T) of lipid nanoparticles at 500 nm ± the standard deviation over 3 measurements.

Particle	%T at 500 nm
BTM_{125}	99.4 ± 0.2
BTM_{65}	75.9 ± 8.1
BTL_{125}	99.2 ± 0.2
BTL_{65}	49.4 ± 2.8